5012 *Organometallics* **2009,** *28,* 5012–5016
DOI: 10.1021/om900542j

ORGANOMETALLICS
Article

Transition Metal Acetylide Rearrangement and Coupling Induced by Coordinative Unsaturation

Chengbao Ni,[†] Gary J. Long,[‡] and Philip P. Power*[,†]

[†]*Department of Chemistry, One Shields Avenue, University of California, Davis, California 95616, and*
[‡]*Department of Chemistry, Missouri University of Science and Technology, University of Missouri,*
Rolla, Missouri 65409-0010

Received June 22, 2009

The reaction of $\{Ar'Fe(\mu\text{-}Br)\}_2$ ($Ar' = C_6H_3\text{-}2,6\text{-}(C_6H_3\text{-}2,6\text{-}^iPr_2)_2$) with $LiC{\equiv}CPh$ afforded the unusual 1,3-butadiene-1,4-diyl Fe(I)-coupled derivative $Fe_2\{Ar'C{=}C(Ph)\text{-}C(Ph){=}CAr'\}$ (**1**), whereas the reaction of $\{Ar'Fe(\mu\text{-}Br)\}_2$ with $LiC{\equiv}C^tBu$ yielded the monomeric Fe(II) "ate" complex $Ar'Fe(C{\equiv}C^tBu)_2\{Li(THF)_2\}$ (**2**). Complexes **1** and **2** were characterized by X-ray crystallography, NMR, and UV−vis spectroscopy and magnetic measurements. In **1** the dimeric structure is a result of Ar′ group transfer to the iron-bound carbon of the acetylide ligand and subsequent dimerization via coupling of the phenyl-substituted carbons. The irons are antiferromagnetically coupled, and the iron−iron separation is 2.5559(3) Å. In **2** the high-spin iron atom has distorted trigonal-planar coordination with a THF-complexed lithium ion associated with the $Ar'Fe(C{\equiv}C^tBu)_2$ anion via interactions with the ^{t}Bu-substituted alkyne carbons.

Introduction

The acetylide group (−C≡CR) group is an extremely versatile ligand, which can bond to one, two, or three transition metal centers in a variety of coordination modes, while donating up to five electrons in bonding.[1−4] Transition metal acetylides have attracted considerable interest for numerous reasons that include their reactivity toward a variety of small molecules to give numerous products,[5−8] metal chalcogenides to form C−E (E = S and Se) bonds,[9,10] or metal carbonyls to yield a variety of clusters.[11] In addition, they display a vast number of insertion and coupling reactions with unsaturated species.[12−23] Acetylide derivatives of iron are well known and are generally stabilized by phosphine, Cp or Cp* (Cp = η^5-C_5H_5; Cp* = η^5-C_5Me_5), or carbonyl co-ligands in high-coordinate complexes (coordination numbers ≥5). Low-coordinate (2 or 3) iron acetylide complexes are rare, but they can be stabilized with use of bulky β-diketiminate co-ligands, as in $HC[C(^tBu)N(2,6\text{-}^iPr_2\text{-}C_6H_3)]_2FeC{\equiv}CR$ (R = $SiMe_3$ or Ph),[24,25] and display single Fe−C bonds to the acetylide group. We have shown that several unusual low-coordinate iron complexes can be synthesized with use of the bulky terphenyl Ar′[26] and related ligands[27] and wished to extend these results to low-coordinate

---

*To whom correspondence should be addressed. E-mail: pppower@ucdavis.edu.

(1) Nast, R. *Coord. Chem. Rev.* **1982**, *47*, 89.
(2) Carty, A. J. *Pure Appl. Chem.* **1982**, *54*, 113.
(3) Sappa, E.; Tiripicchio, A.; Braunstein, P. *Coord. Chem. Rev.* **1985**, *65*, 219.
(4) Raithby, P. R.; Rosales, M. J. *Adv. Inorg. Chem.* **1985**, *29*, 169.
(5) Yi, C. S.; Liu, N. H.; Rheingold, A. L.; LiableSands, L. M.; Guzei, I. A. *Organometallics* **1997**, *16*, 3729.
(6) Kirchbauer, F. G.; Pellny, P. M.; Sun, H. S.; Burlakov, V. V.; Arndt, P.; Baumann, W.; Spannenberg, A.; Rosenthal, U. *Organometallics* **2001**, *20*, 5289.
(7) Bruce, M. I.; Liddell, M. J.; Snow, M. R.; Tiekink, E. R. T. *J. Organomet. Chem.* **1988**, *352*, 199.
(8) Mathur, P.; Ghosh, A. K.; Mukhopadhyay, S.; Srinivasu, C.; Mobin, S. M. *J. Organomet. Chem.* **2003**, *678*, 142.
(9) Mathur, P.; Bhunia, A. K.; Srinivasu, C.; Mobin, S. M. *Phosphorus Sulfur Silicon Relat. Elem.* **2004**, *179*, 899.
(10) Mathur, P.; Srinivasu, C.; Ahmed, M. O.; Puranik, V. G.; Umbarkar, S. B. *J. Organomet. Chem.* **2002**, *659*, 196.
(11) Chi, Y.; Wu, C. H.; Peng, S. M.; Lee, G. H. *Organometallics* **1990**, *9*, 2305.
(12) Jennings, M. C.; Manojlovic-Muir, L.; Puddephatt, R. J. *J. Am. Chem. Soc.* **1989**, *111*, 745.
(13) Benvenutti, M. H. A.; Vargas, M. D.; Braga, D.; Grepioni, F.; Mann, B. E.; Naylor, S. *Organometallics* **1993**, *12*, 2947.
(14) Smith, W. F.; Taylor, N. J.; Carty, A. J. *J. Chem. Soc., Chem. Commun.* **1976**, 896.
(15) Carty, A. J.; Hogarth, G.; Enright, G.; Frapper, G. *Chem. Commun.* **1997**, 1883.
(16) Mathur, P.; Ahmed, M. O.; Kaldis, J. H.; McGlinchey, M. J. *J. Chem. Soc., Dalton Trans.* **2002**, 619.
(17) Rosenthal, U.; Pellny, P. M.; Kirchbauer, F. G.; Burlakov, V. V. *Acc. Chem. Res.* **2000**, *33*, 119.
(18) Shiu, C. W.; Chi, Y.; Chung, C.; Peng, S. M.; Lee, G. H. *Organometallics* **1998**, *17*, 2970.
(19) Busetto, L.; Marchetti, F.; Zacchini, S.; Zanotti, V.; Zoli, E. *J. Organomet. Chem.* **2005**, *690*, 1959.
(20) Maclaughlin, S. A.; Johnson, J. P.; Taylor, N. J.; Carty, A. J.; Sappa, E. *Organometallics* **1983**, *2*, 352.
(21) Onitsuka, K.; Ogawa, H.; Joh, T.; Takahashi, S.; Yamamoto, Y.; Yamazaki, H. *J. Chem. Soc., Dalton Trans.* **1991**, 1531.
(22) Barnea, E.; Andrea, T.; Berthet, J. C.; Ephritikhine, M.; Eisen, M. S. *Organometallics* **2008**, *27*, 3103.
(23) Carty, A. J.; Taylor, N. J.; Lappert, M. F.; Pye, P. L.; Smith, W. F. *J. Chem. Soc., Chem. Commun.* **1978**, 1017.
(24) Vela, J.; Smith, J. M.; Yu, Y.; Ketterer, N. A.; Flaschenriem, C. J.; Lachicotte, R. J.; Holland, P. L. *J. Am. Chem. Soc.* **2005**, *127*, 7857.
(25) Eckert, N. A.; Smith, J. M.; Lachicotte, R. J.; Holland, P. L. *Inorg. Chem.* **2004**, *43*, 3306.
(26) Ni, C. B.; Fettinger, J. C.; Long, G. J.; Power, P. P. *Inorg. Chem.* **2009**, *48*, 2443.
(27) Ni, C. B.; Fettinger, J. C.; Long, G. J.; Brynda, M.; Power, P. P. *Chem. Commun.* **2008**, 6045.

Scheme 1. Proposed Route for the formation of 1[a]

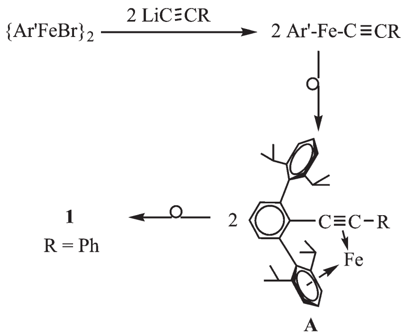

[a] The intermediate **A** appears to be plausible for both R = Ph and ^{t}Bu, but no formation of the ^{t}Bu-substituted coupled species Ar′-C≡C-^{t}Bu complexed or uncomplexed was observed.

Fe(II) acetylides. Herein, we report that the reaction of {Ar′Fe(μ-Br)}$_2$ with LiC≡CPh leads to the unusual coupled 1,3-butadiene-1,4-diyl Fe(I) derivative Fe$_2${Ar′C=C(Ph)-C(Ph)=CAr′} (**1**). In contrast, reaction with LiC≡C^{t}Bu afforded the “ate” complex Ar′Fe(C≡C^{t}Bu)$_2${Li(THF)$_2$} (**2**) with a three-coordinate iron(II) atom.

Result and Discussion

Synthesis. Complexes **1** and **2** were prepared by reaction of the dimer {Ar′Fe(μ-Br)}$_2$ with 2 equiv of the corresponding lithium acetylide salts in a mixture of hexanes and THF (eqs 1 and 2). **1** was isolated as air-sensitive black crystals from hexanes in low yield, while **2** was obtained as extremely air- and moisture-sensitive colorless crystals in good yield. Several attempts were made to obtain a neutral product {Ar′FeC≡C^{t}Bu}$_n$, but only **2** was isolated even when different stoichiometric ratios of {Ar′Fe(μ-Br)}$_2$ with respect to LiC≡C^{t}Bu were used.

$$\{\mathrm{Ar'FeBr}\}_2 + 2\,\mathrm{LiC{\equiv}CPh} \xrightarrow{-\,2\mathrm{LiBr}} \underset{\mathbf{1}}{\mathrm{Fe_2\{Ar'CC(Ph)C(Ph)CAr'\}}} \qquad (1)$$

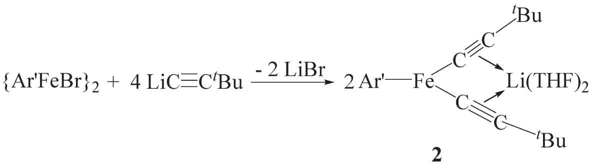

$$\{\mathrm{Ar'FeBr}\}_2 + 4\,\mathrm{LiC{\equiv}C^tBu} \xrightarrow{-\,2\,\mathrm{LiBr}} 2\,\mathrm{Ar'{-}Fe(C{\equiv}C^tBu)_2Li(THF)_2} \qquad (2)$$

2

The mechanism for the formation of **1** is currently unknown. It is possible that the initial step involves elimination of LiBr to afford the Fe(II) intermediate Ar′Fe-C≡CPh. The C−C bond formation between the phenyl acetylide group and the Ar′ ligand may occur to give the alkyne Ar′-C≡C-Ph, which may be complexed to iron via the acetylene group and η^6-complexation of a flanking aryl ring (Scheme 1). Then, oxidative regioselective coupling of the alkyne ligands could occur to form the 1,3-butadiene-1,4-diyl dinuclear iron(I) complex **1**. Such a reaction pathway is similar to the recently reported reactions by zirconium species.[28]

However, this leaves the formation of complex **2** unexplained since, presumably, C−C bond formation between the Ar′ ligand and the -C≡C^{t}Bu group from the initially generated iron(II) intermediate “Ar′Fe-C≡C^{t}Bu” might occur in a similar way to form an Ar′C≡C^{t}Bu/iron complex. However, there is no evidence that such C−C bond formation occurs. Thus, an alternative mechanism (Scheme 2) seems more likely. The initial step involves elimination of LiBr to give the intermediate “Ar′Fe-C≡CPh”, which may associate through the π-donation of the electron-rich acetylide group to the iron(II) ion. In concert with η^6-complexation of the iron by a flanking aryl ring, the Ar′ group then migrates from the iron to form a C−C bond with concomitant reduction of the metal to the +1 oxidation state with generation of radical character at the α-carbon of the acetylide group. The radical generation is facilitated and stabilized by the phenyl substituent at the α-carbon. Radical coupling then leads to dimerization and formation of a C−C bond to afford complex **1**. Nucleophilic attack at the acetylide carbon is also probably favored for the phenyl-substituted species because of its greater charge separation across the acetylide moiety, as evidenced by ^{13}C NMR chemical shift differences.[29] In the case of **2**, it is probable that the ^{t}Bu substituent disfavors Ar′ migration and radical formation because of the charge polarization between the triply bonded carbon atoms in the −C≡C^{t}Bu ligand. The formation of a C−C bond in the final step in Scheme 2 is also sterically disfavored by the large ^{t}Bu substituents. Instead of a rearranged product like **1**, the coordination of another acetylide group to the iron(II) to yield **2** becomes favored.

Scheme 2. Probable Mechanism for the Formation of 1[a]

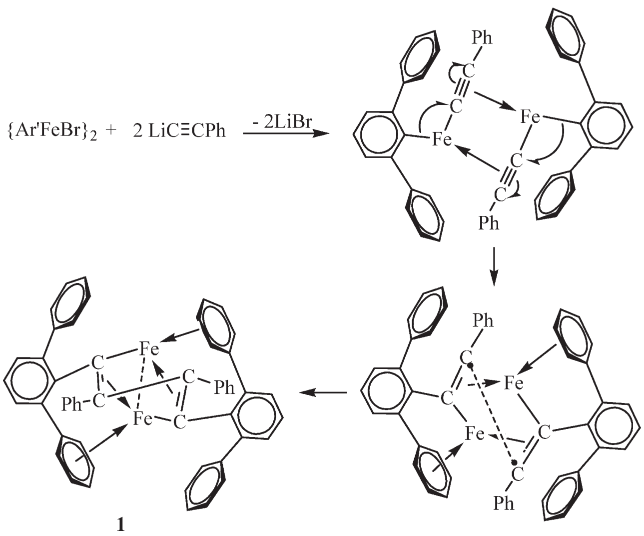

[a] Isopropyl groups on the flanking rings are not shown for clarity.

Spectroscopy. Complex **1** shows a broad, intense absorption centered at 420 nm in the visible region, while complex **2** displays a weak absorption in the ultraviolet region (374 nm) and a featureless spectrum in the visible region. The ^{1}H NMR spectrum of **1** is quite complicated due to the presence of several types of similar hydrogens. At room temperature, slightly broadened signals were observed because of its weak temperature-independent paramagnetism. Due to the η^6-complexation of the C_6H_3-2,6-^{i}Pr$_2$ rings and hindered rotation of the aryl rings, eight sets of doublets and four sets of septets were observed for the ^{i}Pr groups. A feature of the spectrum is that the hydrogen atoms on the η^6-complexed C_6H_3-2,6-^{i}Pr$_2$ and the C_6H_5 rings are dramatically shielded and thus shifted to lower frequencies. This observation is explained by the proximity of the respective

---

(28) Tannaci, J. F.; Kratter, I. H.; Rider, E. A.; McBee, J. L.; Miller, A. D.; Tilley, T. D. *Chem. Commun.* **2009**, 233.

(29) Carty, A. J.; Cherkas, A. A.; Randall, L. H. *Polyhedron* **1988**, *7*, 1045.

Table 1. Selected Crystallographic Data and Collection Parameters for 1 and 2

	$\mathbf{1}\cdot C_6H_{14}$	$\mathbf{2}\cdot C_4H_8O$
formula	$C_{82}H_{98}Fe_2$	$C_{54}\ H_{79}FeLiO_3$
fw	1195.30	838.96
color habit	black plate	colorless block
cryst syst	triclinic	monoclinic
space group	$P\bar{1}$	$P2_1$
a, Å	11.6492(6)	12.4091(14)
b, Å	12.4385(7)	16.2562(19)
c, Å	23.9709(13)	12.4153(14)
α, deg	79.751(1)	90
β, deg	84.532(1)	90.277(2)
γ, deg	70.723(1)	90
V, Å^3	3223.8(3)	2504.4(5)
Z	2	2
d_{calcd}, Mg/m^3	1.231	1.113
θ range, deg	2.90−27.56	2.81−27.11
μ, mm^{-1}	0.495	0.340
obsd data, $I > 2\sigma(I)$	11 792	10 782
R_1(obsd data)	0.0367	0.0398
wR_2(all data)	0.0937	0.1038

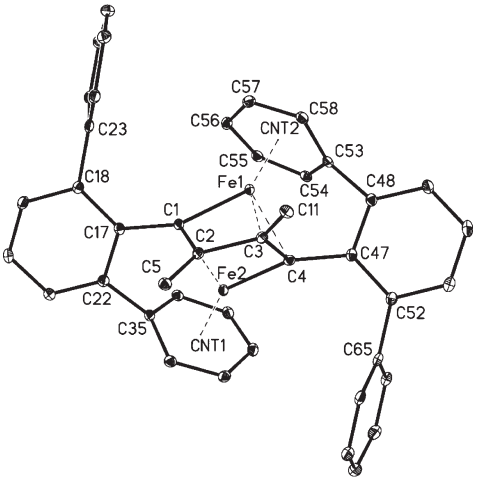

Figure 1. Thermal ellipsoid (30%) plot of **1**. C5 and C11 denote the two phenyl substituents. H atoms and isopropyl groups are not shown. Selected bond lengths (Å) and angles (deg): Fe1---Fe2 2.5559(3), Fe1−C1 1.965(2), Fe1−C3 2.128(2), Fe1−C4 2.058(2), Fe1-Cnt2 1.589(3), C1−C17 1.504(2), C1−C2 1.422(2), C2−C3 1.533(2), C2−C5 1.493(2), C3−C4 1.420(2), C4−C47 1.502(2), C53−C54 1.445(2), C53−C58 1.436(2), C54−C55 1.406(2), C55−C56 1.403(2), C56−C57 1.414(2), C57−C58 1.409(2), C2−C1−C17 119.5(2), Fe1−C1−C17 144.5(1), Fe1−C1−C2 95.9(1), C1−C2−C3 107.0(2), C1−C2−C5 131.1(2), C3−C2−C5 120.2(2), C48−C53−cnt2 163.0.

H atoms to the other aromatic rings. Similarly, some of the isopropyl hydrogens were also shifted to lower frequencies. The ^{1}H NMR spectrum of **2** at room temperature features very broad signals in the range −35 to +30 ppm, which is consistent with the high-spin d^6 electron configuration.

Structures. The structures of **1** and **2** were determined by X-ray crystallography. Important data collection and refinement parameters are provided in Table 1.

The structure of **1** is illustrated in Figure 1. Unlike the normal planar geometry of the five-membered C_4M ring and unequal metal centers observed in metallacyclopentadiene complexes,[28,30−33] which are usually formed via coupled alkynes, complex **1** shows a rather distorted geometry of the C_4M ring and similar iron(I) environment. Binuclear transition metal complexes with 1,3-butadiene-1,4-diyl ligands are rare, and structurally characterized examples are limited to $\{ArN{=}C(H)C(H){=}NAr\}_2Ni_2\{(H)C{=}C(CH_2OCH_3)\}_2$ (Ar = C_6H_3-2,6-^{i}Pr$_2$)[34] and $Rh_2\{\mu_2,\eta^5,\eta^2,\eta^2,\eta^5$-(3-$C_6H_5$-$C_5H_3$)-$(CH_2)_3$-C=C(^{t}Bu)C(^{t}Bu)=C$(CH_2)_3$-(3-$C_6H_5$-$C_5H_3$)$\}$,[35] which were also prepared by alkyne coupling. The Fe···Fe separation in **1** is 2.5559(3) Å, which is slightly longer than the sum (2.48 Å) of the single-bond covalent radii for iron.[36] However, magnetic studies (see below) indicate that the two irons are antiferromagnetically coupled rather than single bonded. The chemical environments of the two iron centers are very similar, so the rest of the discussion focuses on Fe(1). The Fe(1) atom is η^1-σ-bonded to C(1) and η^2-π-bonded to C(3) and C(4) of the 1,3-butadiene-1,4-diyl moiety. In addition, it is η^6-bonded to one of the flanking C_6H_3-2,6-^{i}Pr$_2$ rings of the Ar′ unit attached to C(4). The Fe−C(1) σ-bonded distance, 1.965(2) Å, is slightly longer than that in the butadienyl complex $[Fe_2(CO)_5\{\mu$-η^2,η^3-$H_2C{=}C(Me)C{=}CH_2\}(\mu$-$PPh_2)]$ (1.929(2) Å)[37] and is similar to that in $[Fe_2(CO)_6\{\mu$-η^2-MeCC(NEt$_2$)C(O)Ph$\}]$ (1.964(3) Å).[38] The Fe-η^2 interactions with the double-bonded carbon atoms (C(3) and C(4)) are slightly different (2.128(2) and 2.058(2) Å). The single C(2)−C(3) bond and the double C(1)−C(2) and C(3)−C(4) bonds within the 1,3-butadiene-1,4-diyl ligand are elongated by ca. 0.07 Å compared to uncomplexed 1,3-butadiene molecules.[39−41] The Fe−centroid distances are 1.589(3) and 1.595(3) Å, which are considerably shorter than those in the Fe(I) complexes, such as Ar′FeFeAr′ (1.733(2) and 1.763(2) Å),[42] (η^6-C_6H_6)FeAr*-3,5-^{i}Pr$_2$ (Ar*-3,5-^{i}Pr$_2$ = C_6H-2,6-(C_6H_2-2,4,6-^{i}Pr$_3$)$_2$-3,5-^{i}Pr$_2$, 1.643(2) Å),[43] and [{(C_6H_3-2,6-^{i}Pr$_2$)NC(Me)}$_2$CH]Fe(η^6-C_6H_6) (1.6245(8) Å).[44] The Fe(1)−C(carbon atoms of C(53) aryl ring) distances are in the range 2.050(2) to 2.192(2) Å. The strengths of the metal−carbon interactions to C(53) and C(56) are reflected in the C−C distances involving these atoms (for example, C(53)−C(54) = 1.445(2) Å and C(53)−C(58) = 1.436(2) Å), which are on average 0.02−0.03 Å longer than the other C−C distances within the C(53) aryl ring, and in their deviations from the C54−C55−C57−C58 plane by ca. 0.146 and 0.076 Å, respectively. As a result, the C(57) aryl

---

(30) Hock, A. A.; Mills, O. S. *Acta Crystallogr.* **1961**, *14*, 139.

(31) Bonrath, W.; Michaelis, S.; Porschke, K. R.; Gabor, B.; Mynott, R.; Kruger, C. *J. Organomet. Chem.* **1990**, *397*, 255.

(32) Todd, L. J.; Hickey, J. P.; Wilkinson, J. R.; Huffman, J. C.; Folting, K. *J. Organomet. Chem.* **1976**, *112*, 167.

(33) Dettlaf, G.; Weiss, E. *J. Organomet. Chem.* **1976**, *108*, 213.

(34) Diercks, R.; Stamp, L.; Kopf, J.; Dieck, H. T. *Angew. Chem., Int. Ed. Engl.* **1984**, *23*, 893.

(35) Schaefer, C.; Gleiter, R.; Rominger, F. *J. Organomet. Chem.* **2007**, *692*, 4281.

(36) Pauling, L. *Proc. Natl. Acad. Sci.* **1976**, *73*, 4290.

(37) Breckenridge, S. M.; Maclaughlin, S. A.; Taylor, N. J.; Carty, A. J. *J. Chem. Soc., Chem. Commun.* **1991**, 1718.

(38) Crocq, V.; Daran, J. C.; Jeannin, Y. *J. Organomet. Chem.* **1989**, *373*, 85.

(39) Yamaguchi, S.; Endo, T.; Uchida, M.; Izumizawa, T.; Furukawa, K.; Tamao, K. *Chem.—Eur. J.* **2000**, *6*, 1683.

(40) Bats, J. W.; Urschel, B. *Acta Crystallogr. Sect. E* **2006**, *62*, O748.

(41) Jaroschik, F.; Nief, F.; Le Goff, X. F.; Ricard, L. *Organometallics* **2007**, *26*, 1123.

(42) Nguyen, T.; Merrill, W. A.; Ni, C.; Lei, H.; Fettinger, J. C.; Ellis, B. D.; Long, G. L.; Brynda, M.; Power, P. P. *Angew. Chem., Int. Ed.* **2008**, *47*, 9115.

(43) Ni, C.; Ellis, B. D.; Fettinger, J. C.; Long, G. J.; Power, P. P. *Chem. Commun.* **2008**, 1014.

(44) Smith, J. M.; Sadique, A. R.; Cundari, T. R.; Rodgers, K. R.; Lukat-Rodgers, G.; Lachicotte, R. J.; Flaschenriem, C. J.; Vela, J.; Holland, P. L. *J. Am. Chem. Soc.* **2006**, *128*, 756.

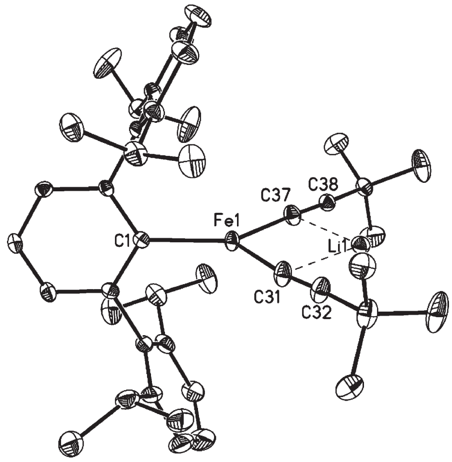

Figure 2. Thermal ellipsoid (30%) plot of **2**. THF molecules bound to lithium and H atoms are not shown. Selected bond lengths (Å) and angles (deg): Fe1−C1 2.039(2), Fe1−C31 2.029(3), Fe1−C37 2.033(2), C31−C32 1.204(4), C1−Fe1−C31 125.6(1), C1−Fe1−C37 130.1(1), C31−Fe1−C37 104.3(1), Fe1−C31−C32 172.5(3).

ring has a distorted boat geometry. Similar distortions are also observed in the central aryl ring of the terphenyl ligand.

The structure of **2** (Figure 2) shows that two acetylide groups become coordinated to the iron atom. There is a lithium ion that is complexed by two THF molecules and two α-carbons from the acetylide moieties to afford an oxidation state of +2 for iron. The iron is terminally bound to an Ar′ ligand and has a distorted trigonal-planar geometry. The Fe−C(1) bond length of 2.039(2) Å resembles the terminal Fe−C distance in the three-coordinate Fe(II) complex $\{Fe(Mes)(\mu\text{-}Mes)\}_2$ (Mes = C_6H_2-2,4,6-Me_3, 2.023(5) Å).[45] The Fe−C(acetylide) distances (2.029(3) and 2.033(2) Å) are essentially equal, but they are somewhat longer than those in other three-coordinate Fe(II) acetylide complexes, such as $HC[C(^tBu)N(2,6\text{-}^iPr_2\text{-}C_6H_3)]_2FeC{\equiv}CR$ (R = $SiMe_3$ 1.961(6) Å;[24] R = Ph, 2.000(2) Å[25]). The torsion angle between the central aryl ring and the C(31)−Fe(1)−C(37) plane is 96.4(2)°. Due to the coordination to the acetylide group to the Li^+ ion, the Fe(1)−C(31)−C(32) angle, 172.5(3)°, deviates slightly from linearity.

Magnetic Studies. The magnetic properties of **1** (Figure 3) indicate that it contains two iron(I) ions that display intramolecular antiferromagnetic exchange with $S = 3/2$, $g = 2$, $J = -186(14)$ cm^{-1} and $N\alpha = 0.00036(8)$ emu/mol Fe. In both plots shown in Figure 3, the solid line through the data points corresponds to the total fit between 30 and 320 K with the $\mathscr{H} = -2J(\boldsymbol{S}_1\cdot\boldsymbol{S}_2)$ Hamiltonian for exchange-coupled dimers.[46,47] The fit also indicates that the sample of **1** studied is 98.2(1) wt % pure. Below ca. 30 K the influence of zero-field splitting or intermolecular exchange interactions, or both, is observed.

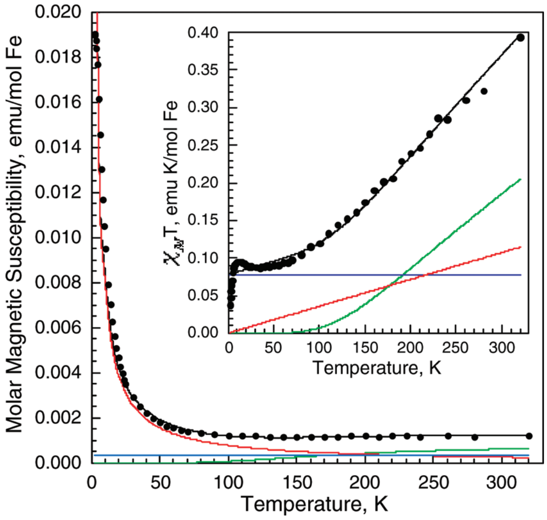

Figure 3. Plot of χ_M versus T for **1**. Inset: $\chi_M T$ versus T of **1**. In both plots the solid line denotes the total fit from 30 to 320 K with $S = 3/2$, $g = 2$, $J = -186(14)$ cm^{-1}, the green component, and $N\alpha = 0.00036(8)$ emu/mol Fe, the blue component, for a sample of **1** that is 98.2(1) wt % pure. The red component is 1.8(1) wt % of a paramagnetic high-spin iron(III) impurity with $S = 5/2$ and a μ_{eff} of 5.92 μ_B.

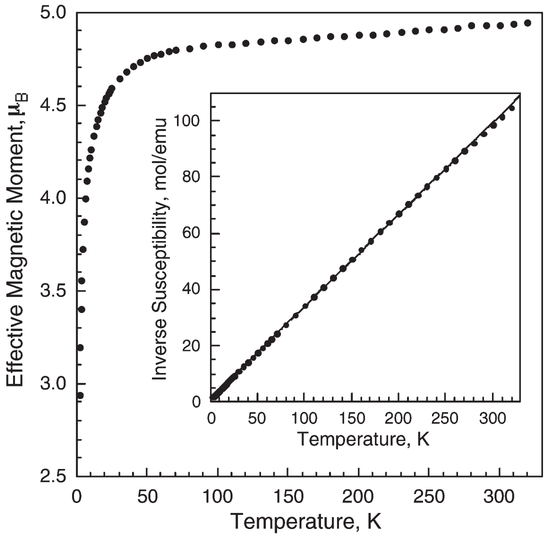

Figure 4. Plot of μ_{eff} versus T for **2**. Inset: plot of $1/\chi_M$ versus T of **2** and a linear Curie−Weiss law fit between 2 and 320 K.

The magnetic properties of **2** (Figure 4) indicate that it is a magnetically dilute high-spin iron(II) complex with $S = 2$ and extensive zero-field splitting as a result of the low-symmetry of the iron(II) coordination environment. As would be expected, the inverse molar magnetic susceptibility ($1/\chi_M$) of **2** (the inset to Figure 4) is linear between 2 and 320 K. A Curie−Weiss fit of $1/\chi_M$ between 2 and 320 K yields a Weiss temperature of −4.1 K, a Curie constant of 3.062 emu K/mol, and a corresponding effective magnetic moment of 4.95 μ_B, which is close to the spin-only value. The lack of significant orbital contribution to the magnetic moment is consistent with the approximate trigonal-planar coordination geometry at Fe(II). For a high-spin d^6 configuration, the d_{z^2} orbital lies lowest and is doubly occupied, while the next highest d_{xz} and d_{yz} orbitals (approximately degenerate) are each singly occupied. The highest $d_{x^2-y^2}$ and d_{xy} orbitals (also approximately degenerate) are also singly occupied. Thus, no vacant degenerate equivalent position with the same spin exists upon rotation of these

---

(45) Muller, H.; Seidel, W.; Gorls, H. *J. Organomet. Chem.* **1993**, *445*, 133.

(46) Details of the Hamiltonian used for this fit are given in the Supporting Information provided in ref 47.

(47) Wolf, R.; Ni, C.; Nguyen, T.; Brynda, M.; Long, G. J.; Sutton, A. D.; Fischer, R. C.; Fettinger, J. C.; Hellman, M.; Pu, L. H.; Power, P. P. *Inorg. Chem.* **2007**, *46*, 11277.

orbitals. As a result of this, orbital angular momentum is quenched.[48]

Experimental Section

General Procedures. All manipulations were carried out using modified Schlenk techniques under an argon atmosphere or in a Vacuum Atmospheres HE-43 drybox. All solvents were dried over an alumina column, followed by storage over 3 Å molecular sieves overnight, and degassed three times (freeze−thaw) prior to use. The metal halide precursors[49] and LiC≡CR (R = Ph or ^{t}Bu)[50] were prepared according to literature procedures. The C and H analyses of **1** were lower than the calculated values due to partial desolvation. Melting points were recorded in glass capillaries sealed under N_2 and are uncorrected. UV−vis data were recorded on a Hitachi-1200 spectrometer. ^{1}H NMR spectra were recorded on a Mercury 300.08 MHz spectrometer at 20 °C.

$Fe_2\{Ar'CC(Ph)C(Ph)CAr'\}\cdot C_6H_{14}$ ($1\cdot C_6H_{14}$). A mixture of hexanes (30 mL) and THF (2 mL) was added to a mixture of $\{Ar'Fe(\mu\text{-}Br)\}_2$ (0.267 g, 0.25 mmol) and LiC≡CPh (0.057 g, 0.53 mmol) at room temperature. The amber solution became deep brown immediately. The mixture was stirred for one day, by which time the solution had become a deep brown color with a brown precipitate. The solution was filtered and concentrated to ca. 10 mL, which afforded X-ray quality, black crystals of **1** after storage for several days at −18 °C. Yield: 0.114 g (41.2%). Mp: 183−185 °C. ^{1}H NMR (300.08 MHz, C_6D_6, 20 °C): δ 0.39 (d, $^3J_{H-H}$ = 6.3 Hz, 6H, $C_aH(CH_3)_2$), 0.75 (d, $^3J_{H-H}$ = 6.3 Hz, 6H, $C_aH(CH_3)_2$), 0.86 (d, $^3J_{H-H}$ = 6.3 Hz, 6H, $C_bH(CH_3)_2$), 1.26 (d, $^3J_{H-H}$ = 6.3 Hz, 6H, $C_bH(CH_3)_2$), 1.36 (d, $^3J_{H-H}$ = 6.3 Hz, 6H, $C_cH(CH_3)_2$), 1.41 (d, $^3J_{H-H}$ = 6.3 Hz, 6H, $C_dH(CH_3)_2$), 1.43 (d, $^3J_{H-H}$ = 6.3 Hz, 6H, $C_dH(CH_3)_2$), 1.61 (d, br, 8H, 6H from $C_cH(CH_3)_2$ and 2H from $C_aH(CH_3)_2$), 2.80 (sept, $^3J_{H-H}$ = 6.3 Hz, 2H, $C_bH(CH_3)_2$), 3.15 (sept, $^3J_{H-H}$ = 6.3 Hz, 2H, $C_cH(CH_3)_2$), 3.71 (sept, $^3J_{H-H}$ = 6.3 Hz, 2H, $C_dH(CH_3)_2$), 4.95 (d, $^3J_{H-H}$ = 6.6 Hz, 2H, *m*-Dipp), 5.09 (d, $^3J_{H-H}$ = 6.6 Hz, 2H, *m*-Dipp), 5.50 (t, $^3J_{H-H}$ = 6.6 Hz, 2H, *p*-Dipp), 5.85 (d, $^3J_{H-H}$ = 6.9 Hz, 2H, *o*-C_6H_5), 6.34 (d, $^3J_{H-H}$ = 7.5 Hz, 2H, *o*-C_6H_5), 6.58 (m, 2H, *m*-C_6H_5), 6.69 (m, 2H, *p*-C_6H_5), 6.77 (m, 2H, *m*-C_6H_5), 7.24 (m, 6H, C_6H_3 and Dipp′), 7.54 (m, 6H, C_6H_3 and Dipp′). Anal. Calcd for $C_{82}H_{98}Fe_2$: C, 82.39; H, 8.26. Found: C, 81.88; H, 7.95. UV−vis (hexane, nm [ε, cm^{-1} M^{-1}]): 420 (3500).

$Ar'Fe(C{\equiv}C^tBu)_2\{Li(THF)_2\}\cdot C_4H_8O$ ($2\cdot C_4H_8O$). A mixture of hexanes (30 mL) and THF (2 mL) was added to a mixture of $\{Ar'Fe(\mu\text{-}Br)\}_2$ (0.267 g, 0.25 mmol) and LiC≡C^{t}Bu (0.089 g, 1.00 mmol) at room temperature. The amber solution became brown in ca. 2 h. The mixture was stirred for one day, by which time the solution had become a brown color with a brown precipitate. The solution was filtered and concentrated to ca. 15 mL, which afforded X-ray quality, colorless crystals of **2** after storage for several days at −18 °C. Yield: 0.282 g (75.8%). Mp: 140−142 °C. ^{1}H NMR (300.08 MHz, C_6D_6, 20 °C): δ −33.46 (br), −12.34 (vbr), −1.35 (br), 1.57 (br), 5.19 (vbr), 7.55 (br), 28.50 (br). Anal. Calcd Ffor $C_{54}H_{79}FeLiO_3$: C, 77.30; H, 9.49. Found: C, 77.14; H, 9.26. IR in Nujol mull (cm^{-1}) in KBr: $\nu_{C\equiv C}$ 2017. UV−vis (hexane, nm [ε, cm^{-1} M^{-1}]): 374 (400).

X-ray Crystallographic Studies. Suitable crystals of **1** and **2** were selected and covered with a layer of hydrocarbon oil under a rapid flow of argon. They were mounted on a glass fiber attached to a copper pin and placed in the cold N_2 stream on the diffractometer. X-ray data were collected on a Bruker SMART 1000 diffractometer at 90(2) K using Mo Kα radiation (λ = 0.71073 Å) or on a Bruker SMART Apex II diffractometer at 90(2) K with Mo Kα radiation (λ = 0.71073 Å). Absorption corrections were applied using SADABS.[51] The structures were solved using direct methods and refined by the full-matrix least-squares procedure in SHELXL.[52] All non-hydrogen atoms were refined anisotropically. Hydrogen atoms in both structures were placed at calculated positions and included in the refinement using a riding model.

Magnetic Studies. Powdered samples of **1** and **2** for magnetic study have been sealed under N_2 in a 3 mm diameter quartz tube. The sample magnetization was measured using a Quantum Designs MPMSXL7 superconducting quantum interference magnetometer; in each case the sample was zero-field cooled to 2 K and the long moment was measured upon warming to 320 K in an applied field of 0.01 T. To ensure thermal equilibrium between the sample in the quartz tube and the temperature sensor, the long moment at each temperature was measured after 44, 36, 28, 20, and 12 min intervals over the temperature ranges 2−5, 5−10, 10−25, 25−70, and 70−320 K, respectively. Diamagnetic corrections of −0.000737 and −0.000549 emu/mol, obtained from tables of Pascal's constants, were applied to the measured susceptibility of **1** and **2**, respectively.

Conclusion

In summary, the attempted synthesis of simple Ar′FeC≡CR (R = Ph or ^{t}Bu) derivatives led, in the case of R = Ph, to an unusual binuclear 1,3-butadiene-1,4-diyl Fe(I) complex stabilized by arene interactions. The formation of **1** probably involves coupling between the Ar′ group and −C≡CR followed by oxidative coupling between the alkynes or an alternative mechanism involving acetylide reductive insertion into the Fe−Ar′ bond followed by coupling. In contrast, for R = ^{t}Bu, only the "ate" complex $Ar'Fe(C{\equiv}C^tBu)_2\{Li(THF)_2\}$ (**2**) could be isolated.

Acknowledgment. We thank the National Science Foundation (CHE-0641020) for financial support, Dr. James C. Fettinger for crystallographic assistance, and Peter Klavins for magnetization measurement assistance.

Supporting Information Available: Crystallographic information files (cifs) for **1** and **2** and ^{1}H NMR spectra for **1** and **2**. These materials are available free of charge via the Internet at http://pubs.acs.org.

---

(48) Figgis, B. N. *Introduction to Ligand Fields*; Wiley: New York, 1966.

(49) Sutton, A. D.; Ngyuen, T.; Fettinger, J. C.; Olmstead, M. M.; Long, G. J.; Power, P. P. *Inorg. Chem.* **2007**, *46*, 4809.

(50) Talalaeva, T. V.; Kocheshkov, K. A. *Izv. Akad. Nauk SSSR-Ser. Khim.* **1953**, 392.

(51) *SADABS Version 5.0; an empirical absorption correction program from the SAINTPlus NT*; Bruker AXS: Madison, WI, 1998.

(52) *SHELXL Version 5.1*; Bruker AXS: Madison WI, 1998.